



## Special Feature: Advanced Alloy Design and Processing of Metallic Materials for Weight- and Energy-saving of Automobiles

Research Report

### Effect of Ni Addition on the Interfacial Reaction Between Cu Lead Frame and Sn-Cu Solder

Takashi Maeshima, Hideaki Ikehata and Shinji Mitao

Report received on Apr. 27, 2018

■**ABSTRACT**■ The effects of Ni addition to the lead frame (LF) Cu alloy on the formation behavior of the intermetallic phases and voids in the interfacially reacted region with the Sn-0.7% Cu solder, during exposures at elevated temperatures such as 423 K were investigated. Multi-layered structures consisting of  $\text{Cu}_3\text{Sn}$  and  $\text{Cu}_6\text{Sn}_5$  intermetallic phases and Kirkendall voids were observed in the interfacially reacted region between LF, containing Ni of 0, 0.09, 0.2 and 0.4%, and the solder. Both the amount of voids and thickness of  $\text{Cu}_3\text{Sn}$  layer markedly decreased with an increase of Ni content from 0 to 0.2%. Microstructural observations for the 0.2% Ni added sample revealed that the Ni-rich layer of about 600 nm in thickness was formed in  $\text{Cu}_3\text{Sn}$  along the LF/ $\text{Cu}_3\text{Sn}$  interface. The mechanism of these phenomena was discussed in terms of microstructure, thermodynamics and kinetics of the reactive interdiffusion process.

■**KEYWORDS**■ Cu Alloy, Lead Frame, Soldering, Interface, Diffusion, Thermodynamics, Chemical Potential,  $\text{Cu}_3\text{Sn}$

#### 1. Introduction

Cu alloys are widely used for lead frames (LF) in semiconductor devices, such as power devices in hybrid or electric vehicles. In such devices, the LF and silicon chips are connected with solder. Sn-0.7 wt% Cu alloy (hereinafter, compositions will be given by wt%, unless otherwise stated) is a promising candidate solder to replace Sn-Pb alloys, as it has a lower environmental impact, a relatively high melting point of around 500 K, and sufficient connection strength.

It is known that intermetallic phases, such as  $\text{Cu}_3\text{Sn}$  and  $\text{Cu}_6\text{Sn}_5$ , are formed between the Cu-based LF and solder by interfacial reaction during soldering. During prolonged exposure to temperatures of around 400 K during operation, Kirkendall voids are formed at the LF/ $\text{Cu}_3\text{Sn}$  interface. Kirkendall voids are known to be formed by marked differences in the interdiffusion coefficients of elements.<sup>(1,2)</sup> The formation of dense Kirkendall voids at the LF/ $\text{Cu}_3\text{Sn}$  interface deteriorates the connection strength and reliability of the solder.

Several studies have reported the effects of the addition of alloying elements to the LF Cu alloys or solder on the formation of intermetallic phases and voids.<sup>(3-12)</sup> Significant effects on the thickness

of the intermetallic phases and void formation have been realized by Ni addition to the LF or solder.<sup>(3,9,12)</sup> However, the underlying mechanism is currently not well understood.

In the present study, the effects of Ni addition to the LF Cu alloy on the formation of intermetallic phases and voids in the interfacially reacted region with Sn-0.7% Cu solder were investigated. Detailed microstructural observations by scanning and transmission electron microscopy were carried out to determine the microstructural change, as well as void formation behavior, due to Ni addition.

#### 2. Experimental

The base composition of the LF was Cu-2%Sn-0.15%Zn-0.006%P. The amounts of Ni added were 0, 0.09, 0.2 and 0.4%. A 0.08 mm-thick Sn-0.7%Cu solder foil was set on mechanically and electro-chemically polished 2 mm-thick LF alloy sheets. Soldering was performed at 553 K for 300 s under a  $\text{N}_2$ -4% $\text{H}_2$  atmosphere. Then, the samples were exposed at 423 K for 1000 and 2000 h. The cross-sectional microstructure was observed by scanning electron microscopy (SEM). The void ratio

was defined as the total void length projected to the interface divided by the measured length (**Fig. 1**). Microstructural observations by scanning transmission electron microscopy (STEM) were conducted for a set of samples exposed at 473 K for 700 h, for an accelerated interfacial reaction. Elemental maps were made by an energy dispersive spectroscopic (EDS) detector in the microscope.

### 3. Results

#### 3.1 Change in the Intermetallic Phases and Voids with the Addition of Ni to LF

Cross-sectional microstructures of the interfacially reacted region observed by SEM in the samples with added Ni of 0, 0.09, 0.2 and 0.4% to the LF are shown in **Fig. 2**. These samples were exposed at 423 K for 2000 h. Multi-layered structures were observed in all the samples, consisting of  $\text{Cu}_3\text{Sn}$  and  $\text{Cu}_6\text{Sn}_5$  intermetallic phases. It is noted that numerous voids were formed along the LF/ $\text{Cu}_3\text{Sn}$  interfaces in the Ni-free sample (**Fig. 2(a)**). The number of voids decreased with increasing amount of Ni, as shown in the micrographs. Careful observations revealed that the voids were formed in  $\text{Cu}_3\text{Sn}$  at the LF/ $\text{Cu}_3\text{Sn}$  interfaces (**Figs. 2(a)** and **(b)**). It is also interesting to note that the thickness of the  $\text{Cu}_3\text{Sn}$  appears to decrease with increasing amount of Ni added.

An example SEM image of the as-soldered sample without high temperature exposures is shown in **Fig. 3**. The LF in the sample contains 0.2% Ni. No voids are recognized in the micrograph. This clearly shows that the voids are formed during exposure at

elevated temperatures after soldering. It is also noted that Ni is detected in  $\text{Cu}_6\text{Sn}_5$  in the as-soldered sample.

Variations of the void ratio as a function of Ni content in the LF are shown in **Fig. 4**. A marked decrease in the void ratio with an increase in the Ni content, especially in the range from 0 to 0.2% Ni, is noted. The void ratio increased with the holding time at 423 K, as shown in the figure.

**Figure 5** shows the variation in thickness of the intermetallic phases as a function of Ni content in the LF. It is noted that the thickness of the  $\text{Cu}_3\text{Sn}$  layer decreased and that of the  $\text{Cu}_6\text{Sn}_5$  layer increased with increasing Ni content. The total thickness of the intermetallic phases was not changed significantly

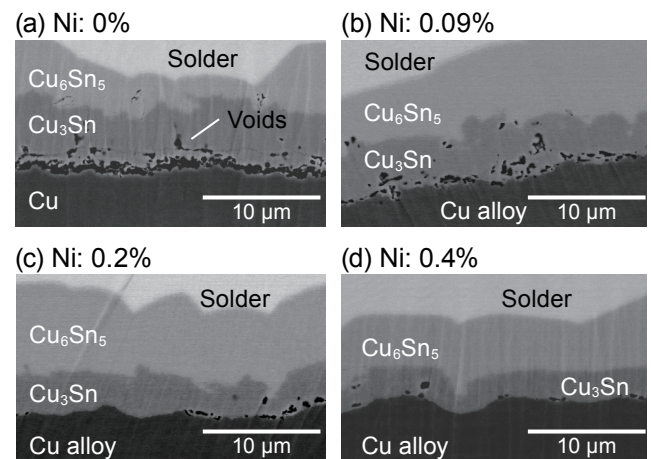
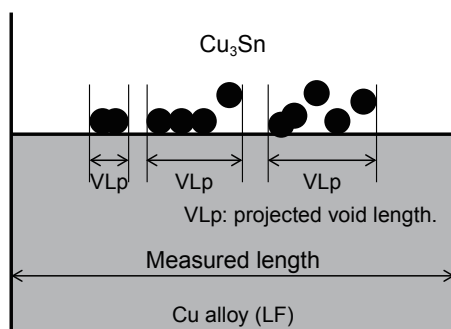


**Fig. 2** SEM images of Cu-xNi/Sn-0.7%Cu solder samples containing (a) 0, (b) 0.09, (c) 0.2, (d) 0.4% Ni, following exposure at 423 K for 2000 h.



$$\text{Void ratio (\%)} = \left[ \frac{\sum (\text{VLP})}{\text{Measured length}} \right] \times 100$$

**Fig. 1** Definition of void ratio.

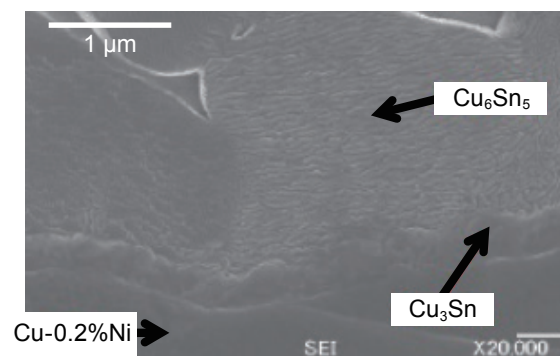


**Fig. 3** Example SEM image of as-soldered sample. The LF contains 0.2% Ni.

with Ni content. The thickness of each phase increased with the holding time at 423 K.

### 3.2 Detailed Microstructural Observations for the 0.2%-Ni-added LF/Cu<sub>3</sub>Sn Interface

Figure 6(a) shows an example high-angle annular dark field (HAADF) image by STEM for the 0.2%-Ni-added LF/Cu<sub>3</sub>Sn interface. The sample was exposed at 473 K for 700 h. An interfacial reaction layer between the LF and Cu<sub>3</sub>Sn with about 600 nm thickness was observed in the micrograph. The distributions of Ni, Cu and Sn detected by EDS in the

same region as for the STEM image are presented in Figs. 6(b), (c) and (d), respectively. It should be noted that Ni is enriched into the interfacial reaction layer between the LF and Cu<sub>3</sub>Sn. It is also noted that the interfacial reaction layer is formed in the Cu<sub>3</sub>Sn side along the interface. The EDS analysis results revealed that the Ni content in the layer was 4.2 at%.

Figure 7(b) shows a selected area diffraction (SAD) pattern acquired from the Ni-rich layer (Fig. 7(a)). The pattern analysis results suggested that the Ni-rich layer was hexagonal (Ni, Cu)<sub>3</sub>Sn,<sup>(12)</sup> although the detected Ni content by EDS was as low as 4.2 at%.

### 4. Discussion

As shown in Fig. 4, the number of Kirkendall voids was markedly decreased with increasing Ni content from 0 to 0.2%. Kirkendall voids were mainly formed in Cu<sub>3</sub>Sn at the LF/Cu<sub>3</sub>Sn interfaces, as seen in Fig. 2. The thickness of the Cu<sub>3</sub>Sn layer also decreased with increasing Ni content, as shown in Fig. 5. The

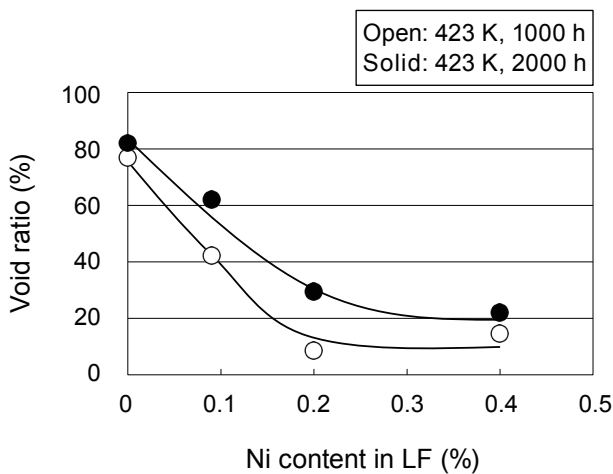


Fig. 4 Variation of void ratio with Ni content in LF.

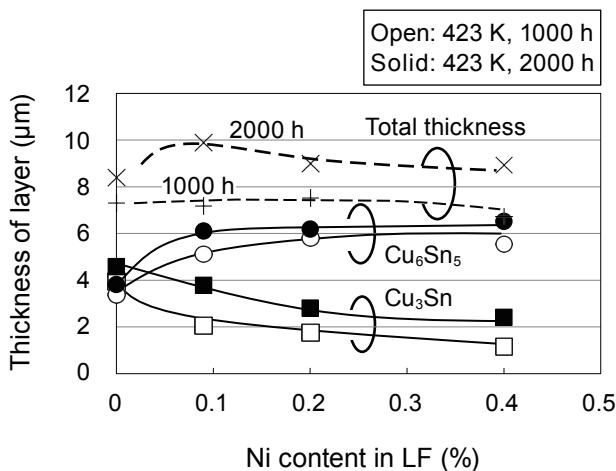


Fig. 5 Thickness of intermetallic phases as function of Ni content in LF.

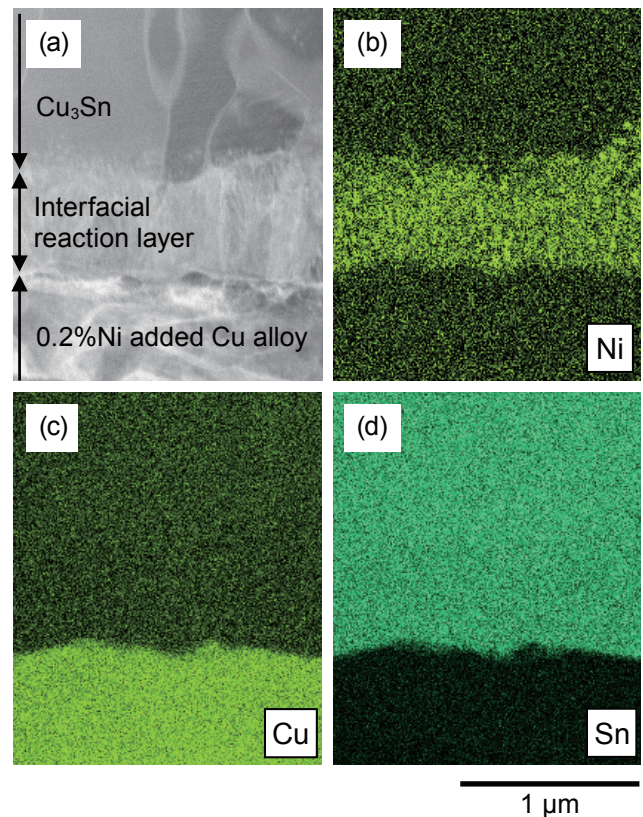


Fig. 6 (a) HAADF image of Cu-0.2%Ni/Cu<sub>3</sub>Sn interface and distribution maps by EDS for (b) Ni, (c) Cu and (d) Sn.

decrease in the number of Kirkendall voids suggests a decrease of inflow of vacancies from the LF to  $\text{Cu}_3\text{Sn}$ , because the diffusion of Sn atoms from  $\text{Cu}_6\text{Sn}_5/\text{Cu}_3\text{Sn}$  becomes comparable to the diffusion of Cu atoms from  $\text{Cu}_3\text{Sn}/\text{LF}$  in  $\text{Cu}_3\text{Sn}$ .

The relationships between the Kirkendall voids, the thicknesses of the  $\text{Cu}_3\text{Sn}$  and  $\text{Cu}_6\text{Sn}_5$  layers and the Ni-rich layer are schematically depicted in Fig. 8. For simplicity, the solder is regarded to be Sn and the LF is regarded to be Cu or Cu-0.2%Ni. Fig. 8(a) shows Ni-free Cu and Fig. 8(b) shows Cu-0.2%Ni. The horizontal axis shows the thickness of the intermetallic phases and the vertical axis shows at% of Sn or Cu. The total thickness of the intermetallic phases is  $8.5\ \mu\text{m}$ , based on the measurement results shown in Fig. 5. The red solid lines are for Cu and the blue ones are for Sn.

In the case of Cu-0.2%Ni, the fraction of  $\text{Cu}_6\text{Sn}_5$  increases, compared with in the case of Ni-free Cu. The broken blue line in Fig. 8(b) represents the profile

of Sn in the intermetallic phases in the case of Ni-free Cu. The amount of Sn included in the  $\text{Cu}_6\text{Sn}_5$  increases with increasing  $\text{Cu}_6\text{Sn}_5$  fraction, which corresponds to the hatched area in Fig. 8(b). Therefore, the number of Kirkendall voids decreases, because the flow of vacancies into  $\text{Cu}_3\text{Sn}$  reduces as shown in Fig. 8(b).

It is known that adding Ni stabilizes the FCC-Cu and  $\text{Cu}_6\text{Sn}_5$  phases, while has almost no effect on the  $\text{Cu}_3\text{Sn}$  phase.<sup>(4,9)</sup> This suggests that adding Ni strongly influences the chemical potential of Sn and Cu in  $\text{Cu}_3\text{Sn}$  assuming local equilibrium at the Cu/ $\text{Cu}_3\text{Sn}$  and  $\text{Cu}_3\text{Sn}/\text{Cu}_6\text{Sn}_5$  interfaces. Rough estimations of the Gibbs free energies for the FCC,  $\text{Cu}_3\text{Sn}$  and  $\text{Cu}_6\text{Sn}_5$  phases in a Sn-Cu binary system are shown in Fig. 9(a). The big difference in the chemical potential of Sn in the  $\text{Cu}_3\text{Sn}$  phase between the  $\text{Cu}_3\text{Sn}/\text{Cu}_6\text{Sn}_5$  ( $\mu_{\text{Sn}}^{\text{Cu}_6\text{Sn}_5/\text{Cu}_3\text{Sn}}$ ) and Cu/ $\text{Cu}_3\text{Sn}$  ( $\mu_{\text{Sn}}^{\text{Cu}/\text{Cu}_3\text{Sn}}$ ) interfaces is noted, suggesting a strong driving force for diffusion of Sn ( $\Delta\mu_{\text{Sn}}^{\text{Cu}_3\text{Sn}}$ ) from  $\text{Cu}_3\text{Sn}/\text{Cu}_6\text{Sn}_5$  to Cu/ $\text{Cu}_3\text{Sn}$  in the  $\text{Cu}_3\text{Sn}$  phase. This is a necessary condition for the

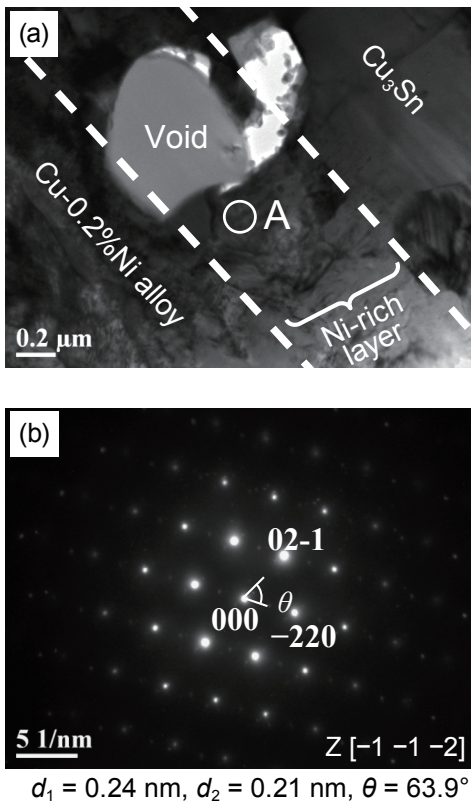


Fig. 7 (a) TEM image showing Ni-rich layer between Cu-0.2%Ni LF and  $\text{Cu}_3\text{Sn}$ . (b) SAD pattern acquired from area A in Fig. 7(a).

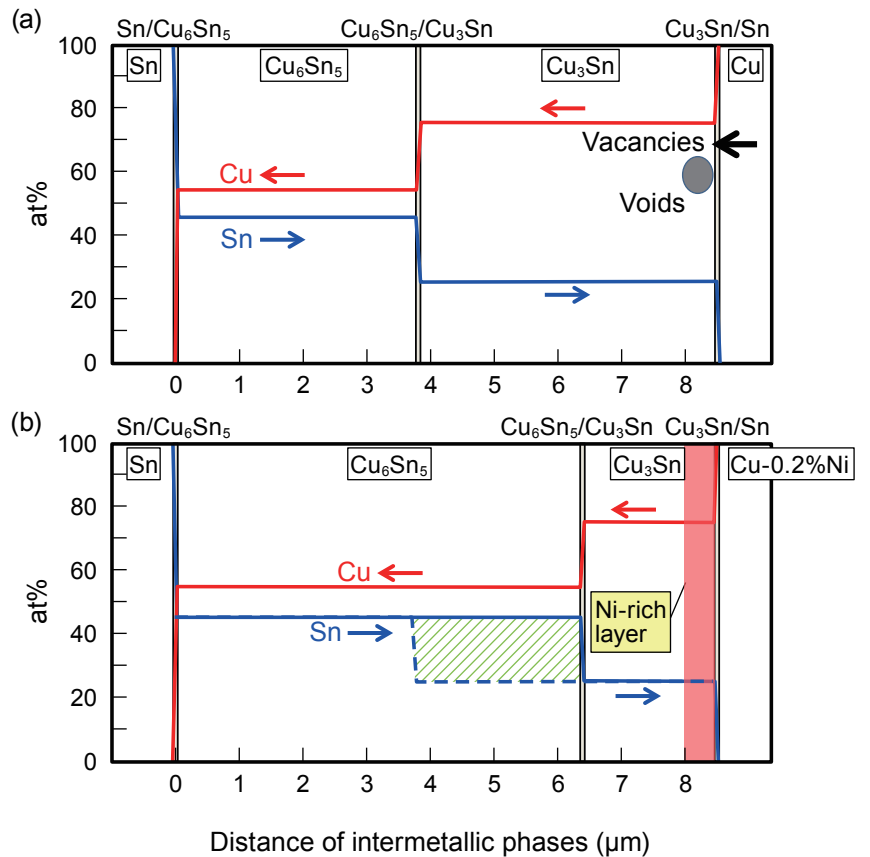
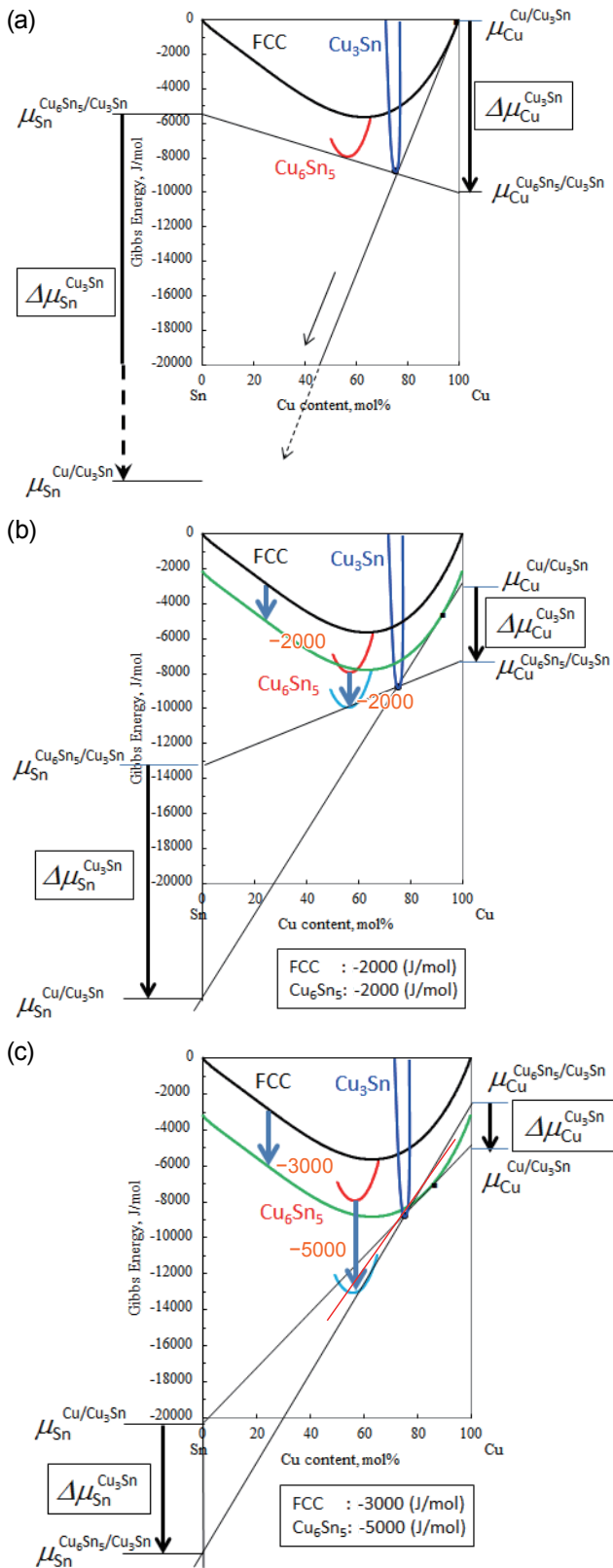


Fig. 8 Schematic diagram representing voids and intermetallic phases in interfacially reacted region between Sn and LF: (a) Ni-free Cu for LF and (b) Cu-0.2%Ni alloy for LF.



**Fig. 9** Schematic illustrations of Gibbs energy curves. (a) Ni-free Cu for LF. (b) Free energy drop assuming  $-2000$  J/mol in FCC and  $\text{Cu}_6\text{Sn}_5$  by Ni addition. (c) Free energy drop assuming  $-3000$  and  $-5000$  J/mol in FCC and  $\text{Cu}_6\text{Sn}_5$ , respectively, by Ni addition.

large flow of Sn from  $\text{Cu}_6\text{Sn}_5$  to the LF in  $\text{Cu}_3\text{Sn}$  as shown in Fig. 8(a).

Figure 9(b) shows the schematic free energy curves assuming a free energy drop of  $2000$  J/mol in the FCC and  $\text{Cu}_6\text{Sn}_5$  phases by Ni addition. The driving force for diffusion of Sn ( $\Delta\mu_{\text{Sn}}^{\text{Cu}_3\text{Sn}}$ ) from  $\text{Cu}_3\text{Sn}/\text{Cu}_6\text{Sn}_5$  to  $\text{Cu}/\text{Cu}_3\text{Sn}$  in the  $\text{Cu}_3\text{Sn}$  phase becomes smaller compared to that in Fig. 9(a). This seems to be a possible factor in the decrease of flow of Sn from  $\text{Cu}_6\text{Sn}_5$  to the LF in  $\text{Cu}_3\text{Sn}$  by Ni addition. In the extreme case, for example, if the free energy of the FCC and  $\text{Cu}_6\text{Sn}_5$  phases drop of  $3000$  and  $5000$  J/mol, respectively, the chemical potential of Sn at the  $\text{Cu}_3\text{Sn}/\text{Cu}_6\text{Sn}_5$  interface ( $\mu_{\text{Sn}}^{\text{Cu}_6\text{Sn}_5/\text{Cu}_3\text{Sn}}$ ) becomes smaller than that at the  $\text{Cu}/\text{Cu}_3\text{Sn}$  interface ( $\mu_{\text{Sn}}^{\text{Cu}/\text{Cu}_3\text{Sn}}$ ) (Fig. 9(c)). In this case, the driving force for diffusion of Sn applies in the opposite direction to the cases represented in Figs. 9(a) and (b), and Sn diffuses from  $\text{Cu}/\text{Cu}_3\text{Sn}$  to  $\text{Cu}_3\text{Sn}/\text{Cu}_6\text{Sn}_5$  in the  $\text{Cu}_3\text{Sn}$  phase. Since the equilibrium of FCC and  $\text{Cu}_6\text{Sn}_5$  is more stable than that of FCC and  $\text{Cu}_3\text{Sn}$ ,  $\text{Cu}_3\text{Sn}$  is considered to disappear at the equilibrium state.

As discussed above, decreases in the free energy of the FCC and  $\text{Cu}_6\text{Sn}_5$  phases by Ni addition are considered to reduce diffusion of Sn from  $\text{Cu}_3\text{Sn}/\text{Cu}_6\text{Sn}_5$  to  $\text{Cu}/\text{Cu}_3\text{Sn}$  in the  $\text{Cu}_3\text{Sn}$  phase, resulting in decreases in the void ratio and the thickness of the  $\text{Cu}_3\text{Sn}$  layer.

The relationships in chemical potential of each phase indicate that the observed Ni-rich layer in Figs. 6 and 7 may have been formed to mitigate the sudden change in chemical potential due to the Ni addition to LF. It seems that considering the phase with thermodynamic calculation, the experimental results were interpreted more suitably as shown in the reference.<sup>(12)</sup> An accurate thermodynamic assessment for Ni-rich phase will be required.

## 5. Conclusions

The effects of Ni addition to a LF Cu alloy on the formation behavior of the intermetallic phases and voids in the interfacially reacted region with Sn-0.7% Cu solder, during exposures at elevated temperatures such as  $423$  K for  $2000$  h, were investigated. The major results lead to the following conclusions:

- (1) Multi-layered structures consisting of  $\text{Cu}_3\text{Sn}$  and  $\text{Cu}_6\text{Sn}_5$  intermetallic phases were observed in the interfacially reacted region between the LF,

containing Ni of 0, 0.09, 0.2 and 0.4%, and the solder.

- (2) Numerous Kirkendall voids were observed in  $\text{Cu}_3\text{Sn}$  at the LF/ $\text{Cu}_3\text{Sn}$  interfaces in the samples containing Ni of 0 and 0.09%. The number of voids markedly decreased with increasing Ni content from 0 to 0.2%.
- (3) The thickness of the  $\text{Cu}_3\text{Sn}$  layer decreased and that of the  $\text{Cu}_6\text{Sn}_5$  layer increased with increasing Ni content, although the total thickness of the intermetallic phases was not changed significantly.
- (4) Detailed microstructural observations for the 0.2%-Ni-added LF/ $\text{Cu}_3\text{Sn}$  interface by TEM revealed that a Ni-rich layer of about 600 nm thickness was formed in  $\text{Cu}_3\text{Sn}$  along the LF/ $\text{Cu}_3\text{Sn}$  interface.
- (5) The decrease of inflow of vacancies from the LF to  $\text{Cu}_3\text{Sn}$  is caused by the changes in thickness of  $\text{Cu}_6\text{Sn}_5$  and  $\text{Cu}_3\text{Sn}$  due to the addition of Ni to LF, resulting in the reduction of Kirkendall voids.
- (6) Thermodynamic considerations suggested that decreases in the free energy of the FCC-Cu and  $\text{Cu}_6\text{Sn}_5$  phases by Ni addition reduced diffusion of Sn from the  $\text{Cu}_3\text{Sn}/\text{Cu}_6\text{Sn}_5$  to Cu/ $\text{Cu}_3\text{Sn}$  interfaces in the  $\text{Cu}_3\text{Sn}$  phase, resulting in decreases in the void ratio and thickness of the  $\text{Cu}_3\text{Sn}$  layer.
- (7) The relationships in chemical potential of each phase indicate that the Ni-rich layer may have been formed to mitigate the sudden change in chemical potential due to the Ni addition to LF.

### Acknowledgments

We acknowledge the assistance of Mr. K. Terui and Mr. Y. Sakamoto of DENSO Corporation in fabricating and analyzing the soldering samples.

### References

- (1) Kirkendall, E., Thomassen, L. and Upthegrove, C., "Rates of Diffusion of Copper and Zinc in Alpha Brass", *Trans. AIME*, Vol. 33 (1939), pp. 186-203.
- (2) Yin, L. and Borgesen, P., "On the Root Cause of Kirkendall Voiding in  $\text{Cu}_3\text{Sn}$ ", *J. Mater. Res.*, Vol. 26, No. 3 (2011), pp. 455-466.
- (3) Nishikawa, H., Piao, J. Y. and Takemoto, T., "Interfacial Reaction between Sn-0.7Cu (-Ni) Solder and Cu Substrate", *J. Electron. Mater.*, Vol. 35, No. 5 (2006), pp. 1127-1132.
- (4) Laurila, T., Hurtig, J., Vuorinen, V. and Kivilahti, J. K., "Effect of Ag, Fe, Au and Ni on the Growth Kinetics of Sn-Cu Intermetallic Compound Layers", *Microelect. Reliability*, Vol. 49, No. 3 (2009), pp. 242-247.
- (5) Yang, L., Zhang, Y., Dai, J., Jing, Y., Ge, J. and Zhang, N., "Microstructure, Interfacial IMC and Mechanical Properties of Sn-0.7Cu-xAl ( $x = 0-0.075$ ) Lead-free Solder Alloy", *Mater. Des.*, Vol. 67 (2015), pp. 209-216.
- (6) Salleh, M. A. A. M., McDonald, S. D., Gourlay, C. M., Belyakov, S. A., Yasuda, H. and Nogita, K., "Effect of Ni on the Formation and Growth of Primary  $\text{Cu}_6\text{Sn}_5$  Intermetallics in Sn-0.7wt%Cu Solder Pastes on Cu Substrates During the Soldering Process", *J. Electron. Mater.*, Vol. 45, No. 1 (2016), pp. 154-163.
- (7) Zeng, G., McDonald, S. D., Gu, Q., Terada, Y., Uesugi, K., Yasuda, H. and Nogita, K., "The Influence of Ni and Zn Additions on Microstructure and Phase Transformations in Sn-0.7Cu/Cu Solder Joints", *Acta Mater.*, Vol. 83 (2015), pp. 357-371.
- (8) Takemoto, T. and Yamamoto, T., "Effect of Additional Elements on Growth Rate of Intermetallic Compounds at Copper/Solder Interface", *J. Jpn. Copper and Brass Res. Ass.* (in Japanese), Vol. 40, No. 1 (2001), pp. 309-316.
- (9) Vuorinen, V., Laurila, T., Mattila, T., Heikinheimo, E. and Kivilahti, J. K., "Solid-state Reactions between Cu (Ni) Alloys and Sn", *J. Electron. Mater.*, Vol. 36, No. 10 (2007), pp. 1355-1362.
- (10) Vuorinen, V., Yu, H., Laurila, T. and Kivilahti, J. K., "Formation of Intermetallic Compounds between Liquid Sn and Various  $\text{CuNi}_x$  Metallizations", *J. Electron. Mater.*, Vol. 37, No. 6 (2008), pp. 792-805.
- (11) Maeshima, T., Ikehata, H., Terui, K. and Sakamoto, Y., "Effect of Ni Addition to Cu Lead Frame on Elemental Diffusion of Solder Joint: Thermodynamically Based Interfacial Reaction Analysis", *Proc. 20th Symp. Microjoining Assem. Technol. Electron.* (in Japanese) (2014), pp. 247-250.
- (12) Maeshima, T., Ikehata, H., Terui, K. and Sakamoto, Y., "Effect of Ni to the Cu Substrate on the Interfacial Reaction with Sn-Cu Solder", *Mater. Des.*, Vol. 103 (2016), pp. 106-113.

Figs. 2 and 6-7

Reprinted from Mater. Des., Vol. 103 (2016), pp. 106-113, Maeshima, T., Ikehata, H., Terui, K. and Sakamoto, Y., Effect of Ni to the Cu Substrate on the Interfacial Reaction with Sn-Cu Solder, © 2016 Elsevier, with permission from Elsevier.

Fig. 9(a)

Reprinted from Proc. 20th Symp. Microjoining Assem. Technol. Electron. (in Japanese) (2014), pp. 247-250, Maeshima, T., Ikehata, H., Terui, K. and Sakamoto, Y., Effect of Ni Addition to Cu Lead Frame on Elemental Diffusion of Solder Joint: Thermodynamically Based Interfacial Reaction Analysis, © 2014 Japan Welding Society.

---

### Takashi Maeshima

Research Fields:

- Additive Manufacturing (AM) Process
- Computational Microstructural Design
- Microscopic Observation and Analysis
- Numerical Heat Transfer Analysis for AM

Academic Degree: Ph.D

Academic Societies:

- The Japan Institute of Metals and Materials
- The Iron and Steel Institute of Japan

Award:

- Mate Best Poster Award, 2013




---

### Hideaki Ikehata

Research Fields:

- Physical Metallurgy
- Metals and Alloys

Academic Societies:

- The Iron and Steel Institute of Japan
- The Japan Society for Heat Treatment
- The Japan Institute of Metals and Materials




---

### Shinji Mitao

Research Field:

- Microstructure-property Relationships in Metallic Materials.

Academic Degree: Dr.Eng.

Academic Societies:

- The Japan Society of Mechanical Engineers
- The Japan Institute of Metals and Materials
- The Iron and Steel Institute of Japan
- Society of Automotive Engineers of Japan

Awards:

- Metallography Award, Best Prize (Category B), The Japan Institute of Metals and Materials, 1996
- Technical Development Award, The Japan Institute of Metals and Materials, 2005, 2009 and 2011
- Nishiyama Commemorative Prize, The Iron and Steel Institute of Japan, 2013
- Industrial Achievement Award, The Japan Institute of Metals and Materials, 2013
- The Invention Award, Japan Institute of Invention and Innovation, 2018

